Xu, H., Chen, H., Halford, N. G., Xu, R., He, T., Yang, B., Zhou, L., Guo, H. and Liu, C. 2025. Ion homeostasis and coordinated salt tolerance mechanisms in a barley (Hordeum vulgare L.) doubled haploid line. *BMC Plant Biology.* 25, p. 52. https://doi.org/10.1186/s12870-024-06033-0

BMC Plant Biology

RESEARCH Open Access

Ion homeostasis and coordinated salt tolerance mechanisms in a barley *(Hordeum vulgare* L.)doubled haploid line

Hongwei Xu[1†], Hui Chen[1†], Nigel G. Halford[2], RugenXu[3], Ting He[1], Bangwei Yang[1], Longhua Zhou[1], HuiminGuo[1*] and ChenghongLiu[1*]

Abstract

Salinization poses a significant challenge in agriculture. Identifying salt-tolerant plant germplasm resources and understanding their mechanisms of salt tolerance are crucial for breeding new salt-tolerant plant varieties. However, one of the primary obstacles to achieving this goal in crops is the physiological complexity of the salt-tolerance trait. In a previous study, we developed a salt-tolerant barley doubled haploid (DH) line, designated as DH20, through mutagenesis combined with microspore culture, establishing it as an idea model for elucidating the mechanisms of salt tolerance. In this study, ion homeostasis, key osmotic agents, antioxidant enzyme activities and gene expression were compared between Hua30 (the original material used as a control) and DH20. The results indicated that under salt treatment, DH20 exhibited significantly higher shoot fresh and dry weight, relative plant height, shoot K^+/Na^+ ratio, improved stomatal guard cell function, and better retention of chloroplast ultrastructure compared to Hua30. Notably, the K^+ efflux in DH20 was significantly lower while the Na^+ and H^+ efflux was significantly higher than those in Hua30 under salt stress in mesophyll cells. Furthermore, the activities of ascorbate peroxidase, superoxide dismutase, and peroxidase, along with the levels of proline, betaine, malondialdehyde, and soluble protein, were correlated with ion efflux and played a vital role in the response of DH20 to salt stress. Compared to Hua30, the relative expression levels of the *HvSOS1*, *HvSOS2*, *HvSOS3*, *HvHKT1;3*, *HvNHX1*, *HvNHX2*, and *HvNHX3* genes, which showed a strong correlation with Na^+, K^+, and H^+ efflux, exhibited significant differences at 24 h under salt stress in DH20. These findings suggest that ion homeostasis, key osmolytes, antioxidant enzyme activities, and associated gene expression are coordinated in the salt tolerance of DH20, with K^+ retention and Na^+ and H^+ efflux serving as important mechanisms for coping with salt stress. These findings present new opportunities for enhancing salinity tolerance, not only in barley but in other cereals as well, including wheat and rice, by integrating this trait with other traditional mechanisms. Furthermore, MIFE measurements of NaCl-induced

†Hongwei Xu and Hui Chen contributed equally to this work as Co-first author.

*Correspondence:
HuiminGuo
guohuimin@saas.sh.cn
ChenghongLiu
liuchenghong@saas.sh.cn

Full list of author information is available at the end of the article

ion fluxes from leaf mesophyll provide plant breeders with an efficient method to screen germplasm for salinity stress tolerance in barley and potentially other crops. Clinical trial number: Not applicable.

Keywords Barley, Salt tolerance, Ion homeostasis, Osmotic agents, Antioxidant enzyme activities, Gene expression

Introduction

Salinization represents one of the most significant challenges in agriculture, particularly in arid and semi-arid regions worldwide [1]. Currently, over 6% of the global land area and 20% of irrigated land are affected by salinization. Projections indicate that by 2050, 50% of the total cultivated land globally will be salinized [2]. In China, the total area of saline soil exceeds 1.0×10^8 hm^2, significantly higher than in other countries [3]. Breeding salt-tolerant plant varieties is the most practical and economical approach to improve agriculture and efficiently utilize saline soil. The main obstacle to achieving this goal in crops lies in the physiological and genetic complexity of the salt-tolerance trait [4, 5].

Barley (*Hordeum vulgare* L.) is recognized as the most salt-tolerant cereal crop worldwide and is among the world's earliest domesticated crop plants [1]. Its simpler genome, superior salt tolerance, rich genetic diversity, and distinct physiological responses make barley a valuable model species for studying salt tolerance. Its comparative advantages over wheat(*Triticum aestivum* L.) and rice (*Oryza sativa* L.) not only enhance our understanding of the underlying mechanisms of salt stress responses but also inform breeding programs aimed at developing more resilient crop varieties capable of thriving in saline environments [1, 6]. Barley has developed various physiological and molecular adaptations to endure salt stress, which are primarily manifested in osmotic regulation, ion balance, antioxidant responses and gene regulation [6]. These include efficient regulation of xylem Na^+ loading, vacuolar Na^+ sequestration, K^+ retention in the cytosol, as well as the management of stomata patterning and function [7].

Among various agronomic traits, the K^+/Na^+ ratio of the entire tissue is recognized as one of the most important parameters for evaluating salt-resistant materials; however, the ion efflux rates of K^+ and Na^+ in mesophyll and root cells should not be overlooked [8]. Recently, non-invasive microelectrode ion flux estimation (MIFE) technology has garnered significant attention due to its advantages of high sensitivity, real-time detection, and non-destructive measurement, demonstrating great potential for development as a high-throughput breeding tool in plants [8, 9]. Substantial progress has been made in studying the physiological mechanisms underlying salt tolerance in barley roots using this technology [10]. A major QTL conferring ROS control of ion flux in roots that coincided with the major QTL for the overall salinity stress tolerance based on MIFE has been observed [11]. This method has revealed that root vacuolar Na^+ sequestration plays a crucial role in the salt tolerance of barley [5]. The effects of calcium, cations, amino acids, and 24-epibrassinolide (EBL) on ion flux and accumulation in barley roots have also been documented [12–15]. Additionally, the relationship between barley xylem ions and salt tolerance has been explored [16]. Furthermore, genes associated with root ion flux have been identified; for instance, *HvHKT1;1* is essential for regulating barley root growth as well as the fluxes of K^+, H^+, and Ca^{2+} under salt stress [17], while vacuolar H^+ pyrophosphatase HVP10 has been shown to regulate Na^+ sequestration in root vacuoles, thereby enhancing H^+ efflux and K^+ retention in the roots [18]. Reports concerning leaves are less frequent. Two studies indicated that K^+ retention in leaf mesophyll is critical for the salt tolerance of barley [8, 19]. However, no reports have compared the efflux rates of Na^+, K^+, and H^+ in different tissues of a barley doubled haploid (DH) line created through mutagenesis combined with microspore culture under salt stress.

When compared to traditional breeding methods, the use of double haploid (DH) lines derived from microspore culture presents several distinct advantages. These include the ability to achieve rapid homozygosity, simplify breeding operations, enhance selection efficiency, facilitate marker-assisted selection, improve hybrid development, integrate genomic tools, preserve genetic diversity, reduce of environmental influence and cost-effectiveness [20–22]. In many species, doubled haploids can be produced via isolated microspore or anther culture [23]. Compared to anther culture, microspores due to the free of anther wall tissues is totipotency, which makes them an excellent haploid model to produce DH plants [24]. In the early stages of this study, we developed a salt-tolerant doubled haploid (DH) line (DH20) through microspore mutagenesis in barley [25]. The mutant materials were obtained by treating dry seeds of Hua30 with 500 Gy Co-60 gamma irradiation, followed by microspore culture. DH20 were screened from thirty-one DH lines is more stable and heritable than the wild type Hua30, rendering it an ideal resource for elucidating the physiological mechanisms underlying salt tolerance. The integration of transcriptome and metabolome analyses revealed that nine key biomarkers, including two metabolites and seven genes, could distinguish DH20 and H30 when exposed to high salt. Additionally, DH20 exhibited better performance on shoot K^+/Na^+ ratio and key photosynthetic characteristics (A, GS, E and Ci) than the control Hua 30 under salt stress conditions [25].

This research primarily employs the DH20 line to investigate the ion efflux flow rates of K^+, Na^+, and H^+ in mesophyll cells, root epidermal cells, and xylem. Furthermore, it aims to examine the correlation between ion efflux flow rates and osmolytes, as well as the antioxidant enzymes and associated genes. The ultimate goal is to further elucidate the mechanisms of ion regulation that underlie salt tolerance, thereby providing a theoretical foundation for the rapid breeding of salt-tolerant varieties.

Materials and methods

Plant materials and salt treatments

This study included two barley genotypes: Hua30, a widely cultivated barley (*Hordeum vulgare* L.) cultivar in the Yangtze River Delta of China, developed through anther culture from a cross between the spring two-rowed cultivar 'Xiumai1' and the breeding line 'Xiu82-164'; and Double Haploid 20 (DH20), a stable homozygous salt-tolerant line, developed through a combination of physical mutagenesis, microspore culture, and salt tolerance screening derived from Hua30 by the Shanghai Academy of Agricultural Sciences [25]. All seeds were provided by the Shanghai Academy of Agricultural Sciences. Plump and uniform seeds of both Hua30 and DH20 were sterilized with 10% NaClO for 10 min, followed by germination on petri dishes lined with wet filter paper for 4 to 5 days. The seedlings were then cultured in water for one day to facilitate gradual acclimatization to the solution culture, after which they were transferred to Hoagland nutrient solution, which was changed every two days. At the two-leaf stage, seedlings were subjected to treatment with Hoagland solution, one containing 360 mM NaCl to assess their salt tolerance and the other one as the control. The PH of both the control and salt solutions was adjusted to 5.8. Each treatment group consisted of at least ten plants. The assessment of salt tolerance was conducted in a phytotron maintained at a temperature regime of 22 ℃/18°C (light/dark), with a light intensity of 300 μmol m^{-2} s^{-1}, a light/dark cycle of 16/8 hours, and a relative humidity of 70%.

Measurement of the plant growth metrics and the shoot K+/Na+ ratio

After 28d of salt treatment, seedlings were collected to the determine the fresh and dry weights of both shoots and roots. The net photosynthetic rate and Fv'/Fm' were measured using a LI-6800 portable photosynthesis system (LI-COR Inc., Lincoln, USA). The chlorophyll content in the leaves was determined using a SPAD-502 chlorophyll meter (Minolta, Japan). The relative growth rate of plant height was calculated as the (plant height for the corresponding days after treatment—plant height before treatment)/ plant height before treatment). After sampling, the contents of Na^+ and K^+ were determined by an inductively-coupled argon plasma emission spectrometer iCAP6300 instrument (Thermo Scientific, Walthmam, MA, USA). Six biological replicates were used for each measurement.

Estimation of the length of stomatal guard cells

The lengths of stomatal guard cells were determined by the Wuhan Maispu Biotechnology Co., Ltd following the methodology outlined by Li et al. (2022) [26]. After salt treated for 24 h, the middle portion of the top second leaf, measuring 3–4 cm in length, was washed with a phosphate buffer solution (pH 7.2) and fixed in a 2.5% glutaraldehyde solution for 24 h at 4 °C. Subsequently, dehydration was carried out using a stepwise ethanol gradient from 30 to 100% (two times). Finally, the samples were rinsed with distilled water, and the lengths of the stomatal guard cells were measured under a 400× field Olympus microscope (Olympus DP71, Tokyo, Japan). Five stomata per leaf section were randomly selected at fixed points of the middle sections of the upper second leaves and measured from ten different leaves of DH20 and Hua30, respectively.

Chloroplast ultrastructure

The ultrastructure of chloroplasts was detected by modifying the method developed by Wuhan Maispu Biotechnology Co., Ltd, with reference to Moussa et al. (2010) [27] and the book "Electron Microscopy Technology in Life Sciences." The middle sections of the top second leaves were harvested and fixed in 2.5% glutaraldehyde for 2 ~ 4 h at 4℃, and then refixed with 1% osmic acid. After dehydration using a series of ethanol concentrations (30 ~ 100%) for 40 min each, the samples were treated with penetration, embedding, polymerization and staining. The ultrastructure of the chloroplasts was observed under transmission electron microscope (Hitachi High-technologies Corporation, Tokyo, Japan). Five chloroplasts ultrastructure were randomly selected at fixed points of the middle sections of the upper second leaves and measured from ten different leaves of DH20 and Hua30, respectively.

Measurement of the net flux of Na+, K+ and H+

Na^+, K^+ and H^+ efflux and internalization were measured using non-invasive microsensing technology (NMT Physiolyzer®, Younger, USA LLC, Amherst, MA 01002, USA; Xuyue Technology Co., Ltd., Beijing, China). After salt treated for 24 h, barley leaves with an area of 0.3 cm*0.3 cm were cut off, then the mesophyll tissue was exposed and fixed at the bottom of the Petri dish. After then, load the sample to detect the Na^+, K^+ and H^+ flux of the mesophyll tissue. Similarly, the root tissue was

exposed and fixed at the bottom of the Petri dish. After then, load the sample to detect the K^+ and Na^+ flux of the root tissue as well as the Na^+ loading rate of root xylem. Flux data were obtained and output using the software of imFluxes V3.0 (Younger USA LLC, Amherst, MA 01002, USA). According to the Zeng et al. (2024) [28], the sign convention for NMT data was "influx negative" and "efflux positive". For the measurement, mesophyll cell measurements were conducted at the surface of the mesophyll tissue, while root surface measurements were taken in the elongation zone, located 1200 μm from the apical root tip. Additionally, root xylem measurements were performed at a distance of 5000 μm from the apical root tip. A total of ten biological replicates and three technical replicates were randomly selected at fixed points within the mesophyll tissue, elongation zone, and xylem.

Determination of the content of proline, betaine, malondialdehyde, abscisic acid, soluble sugar and soluble protein

The contents of proline, betaine, malondialdehyde (MDA), soluble sugar, and soluble protein were determined following the protocols outlined in the assay kits for proline (M0108A), betaine (M0128A), MDA (M0106A), soluble sugar (M1503A), and soluble protein (M1806A) from Suzhou Michy Biomedical Technology Co., Ltd, Suzhou, China. Briefly, samples weighing 0.1 g were mixed with 1 mL of extraction buffer and then centrifuged at 12,000 rpm for 10 min at 4 °C. The absorbance of the resulting supernatant was measured at wavelengths of 520 nm, 525 nm, 532 nm, 620 nm, and 562 nm using a microplate reader (Spectra Max iD3, Molecular Devices, United States). The concentrations of proline, betaine, MDA, soluble sugar, and soluble protein were expressed as μg/g fresh weight (FW). Approximately 0.5 g of the sample was weighed, and 1.5 mL of precooled 80% methanol aqueous solution was added to create a homogenate, which was maintained in an ice bath overnight. The mixture was then centrifuged at 8000 g for 10 min to obtain the supernatant. Subsequently, 2 mL of petroleum ether was added for extraction and decolorization, repeated twice, after which 0.2 mL of methanol was added to dissolve the residue, mixed, and filtered for testing. The ABA content was determined using a Waters 2695 high-performance liquid chromatograph operating at a wavelength of 254 nm. The analysis utilized a Compass C18 (2) reversed-phase column (250 mm x 4.6 mm, 5 μm) at a column temperature of 35 °C, with a flow rate of 1 mL/min and an injection volume of 10 μL. The mobile phase comprised a 1% acetic acid aqueous solution mixed with methanol in a 60:40 (V/V) ratio. Each treatment sample consisted of three biological replicates and three technical replicates.

Determination of ascorbate peroxidase, catalase, superoxide dismutase and peroxidase

After 24 h of salt stress, fresh leaves from the plants were collected and stored at -80 ℃ for later use. The activities of ascorbate peroxidase (APX, M0403A), catalase (CAT, M0103A), superoxide dismutase (SOD, M0102A) and peroxidase (POD, M0105A), were determined according to the commercial kits (Suzhou Michy Biomedical Technology Co., Ltd, Suzhou, China), respectively. Briefly, samples weighing 0.1 g were homogenized in extraction buffer, followed by centrifugation at 12,000 rpm for 10 min at 4 °C. The resulting supernatants were then collected for the determination of enzyme activities using the above assay kits. The absorbance of the supernatant was measured at 290 nm, 405 nm, 450 nm and 470 nm with a microplate reader (Spectra Max iD3, Molecular Devices, United States), and the activities of APX, CAT, SOD and POD were calculated as nmol/min/g FW, μmol/min/g FW, U/g FW and U/g FW, respectively. Each treatment sample consisted of three biological replicates and three technical replicates.

RNA extraction and quantitative real time PCR

Total RNA was extracted from barley leaves using Trizol reagent (Thermo Scientific, USA) following the manufacturer's instructions. Each treatment sample consisted of three biological replicates and three technical replicates. The primers were designed using Primer 3 plus in NCBI, as detailed in Table S1. The first-strand cDNA was synthesized with the PrimeScript™II 1st Strand cDNA Synthesis Kit (Takara, Japan), according to the manufacturer's instructions. Quantitative PCR (qPCR) reactions were performed on the 7,500 Fast platform (Applied Biosystems, United States) using PowerUp™ SYBR™ Green Master Mix (Applied Biosystems). Each 20-μl reaction contained 10 μl of PowerUp™ SYBR™ Green Master Mix, 2 μl of 5× diluted cDNA, and 0.8 μl of each forward and reverse primer (10 μM). The reaction was predenatured at 50 °C for 20 s, then at 95 °C for 10 min, followed by 40 cycles of 95 °C for 15s and 60 °C for 1 min. For quantification, the comparative CT method (ΔΔCT method) was used to quantify the relative expression of specific genes [29].

Statistical analyses

All data were analyzed using SPSS version 21.0 (SPSS, Chicago, IL, USA). The significance of the correlation between different parameters was assessed using bivariate correlations based on Pearson's correlation (two-tailed). Different lowercase letters denote significant differences between Hua30 and DH20 under different treatments at the 0.05 level, as determined by Fisher's least significant difference (LSD) test [30].

Results

DH20 exhibited higher salinity tolerance in shoots

Under the control treatment, no significant differences were observed in the fresh and dry weights of shoot and root between Hua30 and DH20 (Table 1). However, the fresh weight and dry weight of the shoots in DH20 was significantly higher than that of Hua30 under salt stress. There was no difference in root fresh weight and root dry weight between the two materials under salt stress (Table 1). Furthermore, in response to salt treatment, the maximum net photosynthetic rate、Fv'/Fm'、chlorophyll content、leaf K^+/Na^+ ratio and the relative growth rate of plant height in DH20 were higher than those of Hua30 (Table 1; Fig. 1). Overall, the DH20 and Hua30 used in this study exhibited significant differences in their shoot salt tolerance.

Effect of salt stress on the stomatal guard cells and chloroplast ultrastructure in Hua30 and DH20

In our previous study, DH20 exhibited superior salt tolerance compared to Hua30 regarding photosynthetic characteristics [25]. Here, there was no significant difference in the opening of stomatal guard cells between DH20 and Hua30 under normal conditions. However, under salt stress, the stomatal opening of DH20 was significantly larger than that of Hua30 (Fig. 2A). When comparing the average length of stomatal guard cells, it was found that those of DH20 were significantly longer than those of Hua30 by 55.17% under salt stress. Under control conditions, both Hua30 and DH20 plants exhibited normal chloroplasts with well-developed structures, including normally stacked grana and thylakoid membranes. Following salt stress treatment, Hua30 showed noticeable plasmolysis, with a disordered arrangement of thylakoid lamellae and a fuzzy structure. In contrast, DH20 displayed no significant plasmolysis, and the arrangement of thylakoids remained relatively clear, with only minor changes (Fig. 2B).

Table 1 Comparisons of Hua30 and DH20 for growth and leaf K^+/Na^+ ratio under control and salt stress conditions

Trait	Control		Salt stress	
	Hua30	DH20	Hua30	DH20
Shoot fresh weight(g)	1.76 ± 0.03^a	1.79 ± 0.03^a	0.13 ± 0.02^c	0.23 ± 0.01^b
Root fresh weight(g)	0.34 ± 0.03^a	0.35 ± 0.04^a	0.03 ± 0.002^b	0.05 ± 0.004^b
Shoot dry weight(g)	0.17 ± 0.02^a	0.18 ± 0.02^a	0.02 ± 0.001^c	0.04 ± 0.001^b
Root dry weight(g)	0.03 ± 0.001^a	0.03 ± 0.003^a	0.004 ± 0.00^b	0.005 ± 0.00^b
Maximum net photosynthetic rate ($\mu mol\ m^{-2}\ s^{-1}$)	5.81 ± 0.59^a	6.32 ± 0.52^a	0.95 ± 0.18^c	1.51 ± 0.27^b
Fv'/Fm'	0.50 ± 0.01^a	0.51 ± 0.01^a	0.32 ± 0.04^c	0.45 ± 0.03^b
Leaf chlorophyll content (SPAD)	38.7 ± 2.52^a	39.16 ± 2.68^a	27.51 ± 0.95^c	31.77 ± 2.63^b
Leaf K^+/Na^+ ratio	59.78 ± 3.81^a	62.61 ± 2.35^a	0.24 ± 0.04^c	0.65 ± 0.07^b

Different lowercase letters within the row in table indicate significant differences between Hua30 and DH20 under different treatment at 0.05 levels by Fisher's least significant difference (LSD) test

Comparison of Na+, K+ and H+ effluxes in different tissue of salt-treated Hua30 and DH20

To further investigate the mechanism of salt tolerance, we employed the NMT system to measure the dynamics of ion flux for Na^+, K^+, and H^+. Under salt stress, the flow velocity curves for Na^+ and H^+ efflux in Hua30 consistently exceeded those in DH20 throughout the detection period from 0s to 270s, with the average flow velocities of Na^+ and H^+ efflux being significantly higher in Hua30 (Fig. 3A and C). In mesophyll cells, a comparison of K^+ efflux flow velocities between the two materials revealed that the efflux velocity curves for K^+ in DH20 were consistently lower than those observed in Hua30 during the detection period of 0s to 270s (Fig. 3B). The average flow velocities of K^+ efflux were significantly lower in DH20 (Fig. 3B). In root epidermal cells, no significant differences were observed in the efflux of Na^+ and K^+(Figure 3D and E). However, in root xylem cells, the absorption flux of Na^+ was significantly lower in DH20 compared to Hua30 (Fig. 3F).

Effects of salt stress on the osmolytes and ABA in Hua30 and DH20

The differences in the contents of proline (PRO), betaine, malondialdehyde (MDA), abscisic acid (ABA), soluble sugar, and soluble protein between Hua30 and DH20 were compared. Under salt stress, the levels of PRO and soluble protein in DH20 were significantly higher than those in Hua30 (Fig. 4A and F). Under normal control conditions, no significant difference in MDA levels was observed between Hua30 and DH20; however, under salt stress, DH20 exhibited significantly lower MDA levels than Hua30 (Fig. 4C). Under normal control conditions, the betaine and ABA contents in DH20 were significantly lower than those in Hua30, whereas under salt stress, DH20 showed higher betaine content and no significant difference in ABA levels compared to Hua30 (Fig. 4B and D). There was no significant difference in soluble sugar content between Hua30 and DH20 under both control and salt stress conditions (Fig. 4E).

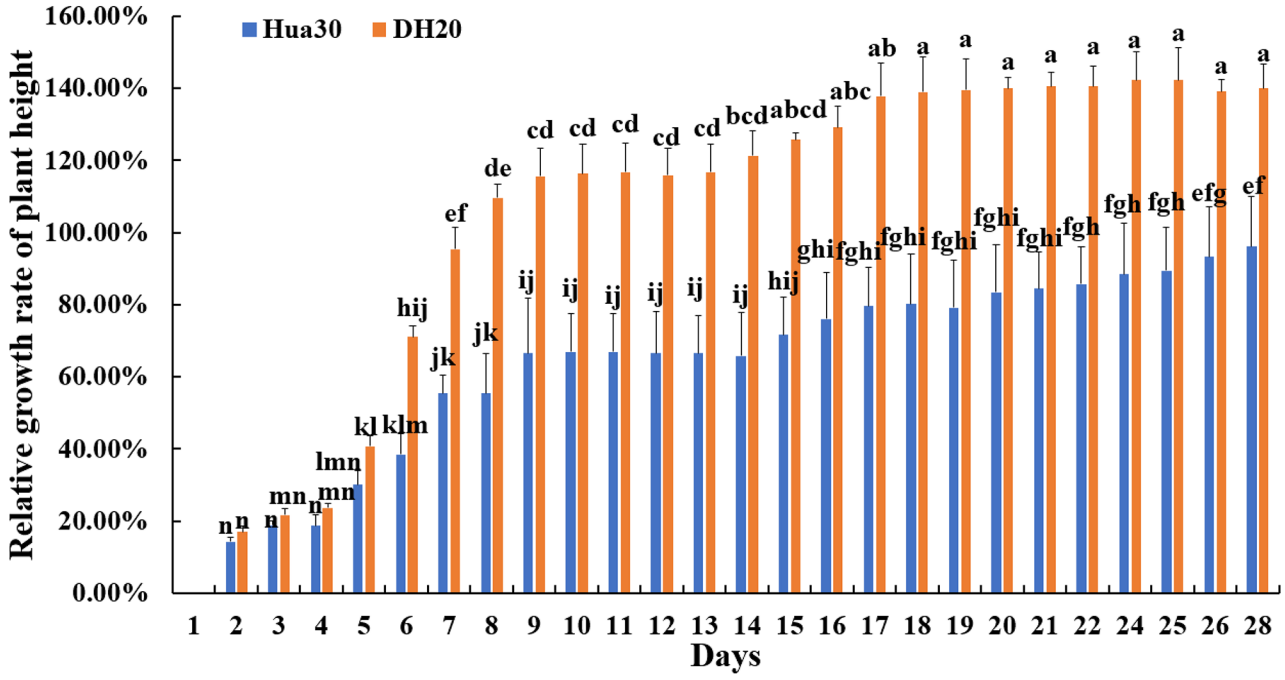

Fig. 1 The relative growth rate of plant height in Hua30 and DH20. The relative growth rate was calculated based on the following formula: relative growth rate (%) = (plant height for the corresponding days after treatment- plant height before treatment)/ plant height before treatment. The different lowercase letters indicate significant differences in the relative growth rate of plant height between Hua30 and DH20 under different treatment at 0.05 levels by Fisher's least significant difference (LSD) test

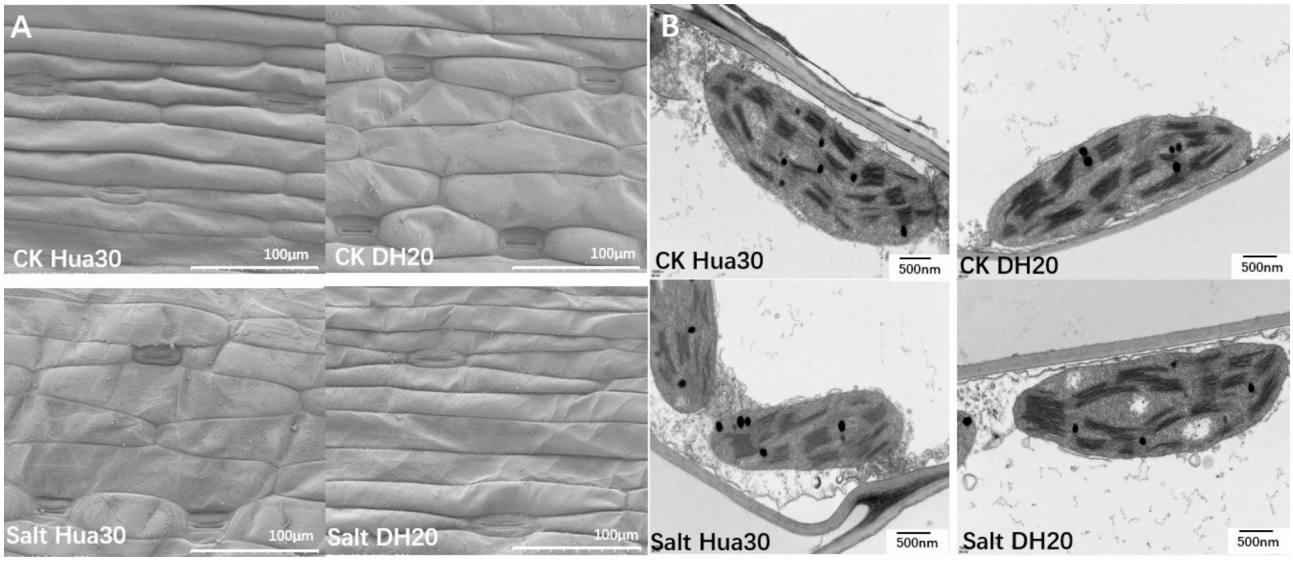

Fig. 2 Comparison of stomatal guard cells (**A**) and chloroplast ultrastructure (**B**) of Hua30 and DH20 under different treatments. **A**: The scale represents 100 μm; **B**: The scale represents 500 nm

To investigate the potential role of osmolytes in the ion efflux rates of Na^+, K^+, and H^+ in mesophyll cells, we compared the correlations among them under salt stress (Fig. 4G). Proline and betaine showed a highly significant correlation with the efflux rates of Na^+, K^+, and H^+. Malondialdehyde (MDA) demonstrated a highly significant correlation with Na^+ efflux, and a significant correlation with K^+ and H^+ efflux rates. Additionally, the K^+ efflux rate exhibited a significant correlation with soluble protein. These findings suggest that the levels of proline, betaine, malondialdehyde and soluble protein are crucial for the response of DH20 to salt stress.

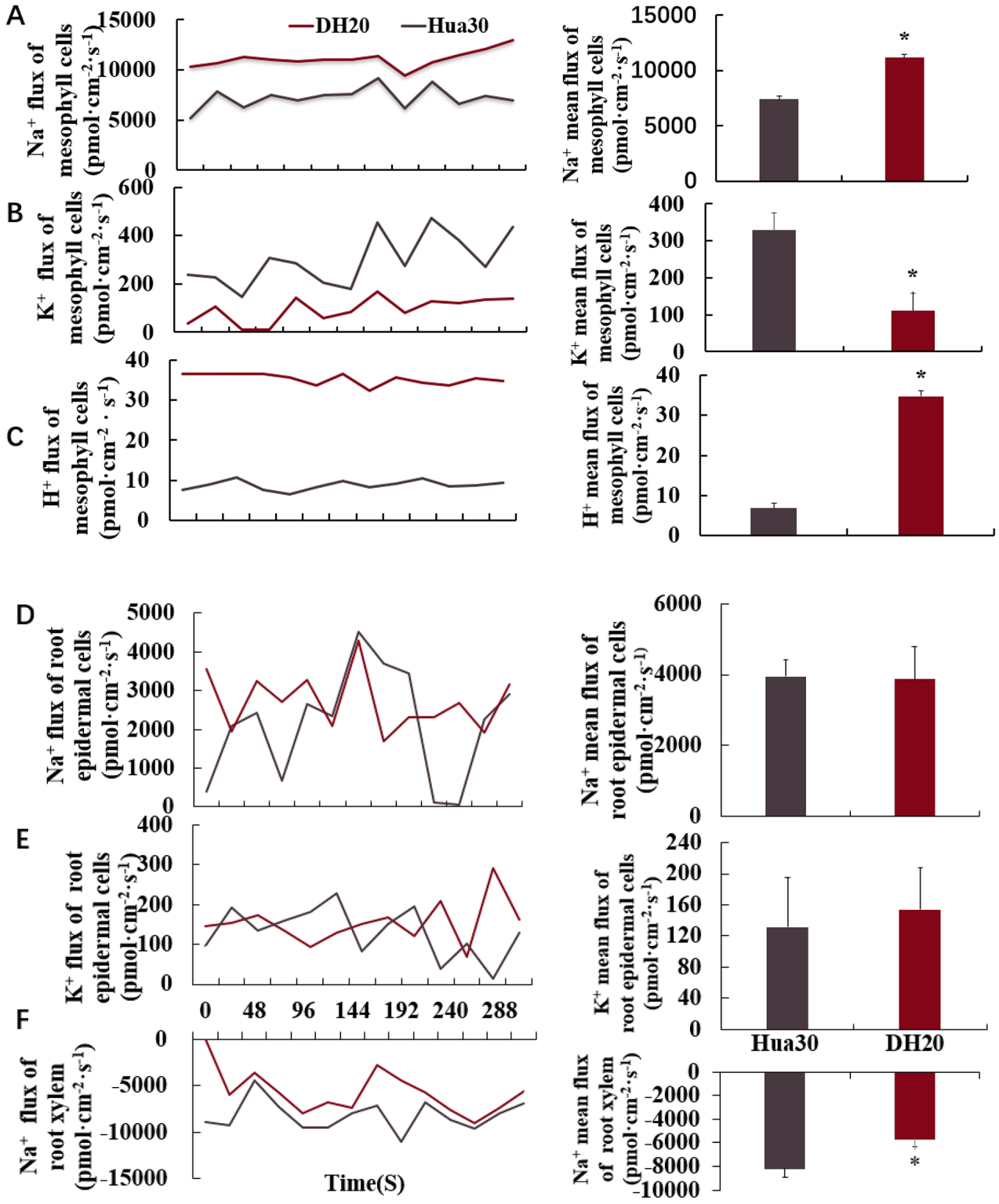

Fig. 3 The efflux of Na^+, K^+ and H^+ in different tissues of Hua30 and DH20 under salt stress. **A**: Na^+ efflux of mesophyll cells; **B**: K^+ efflux of mesophyll cells; **C**: H^+ efflux of mesophyll cells; **D**: Na^+ efflux of root epidermal cells; **E**: K^+ efflux of root epidermal cells; **F**: Na^+ efflux of root xylem cell. Asterisk (*) represent a significant difference between the two materials at the 0.05 level

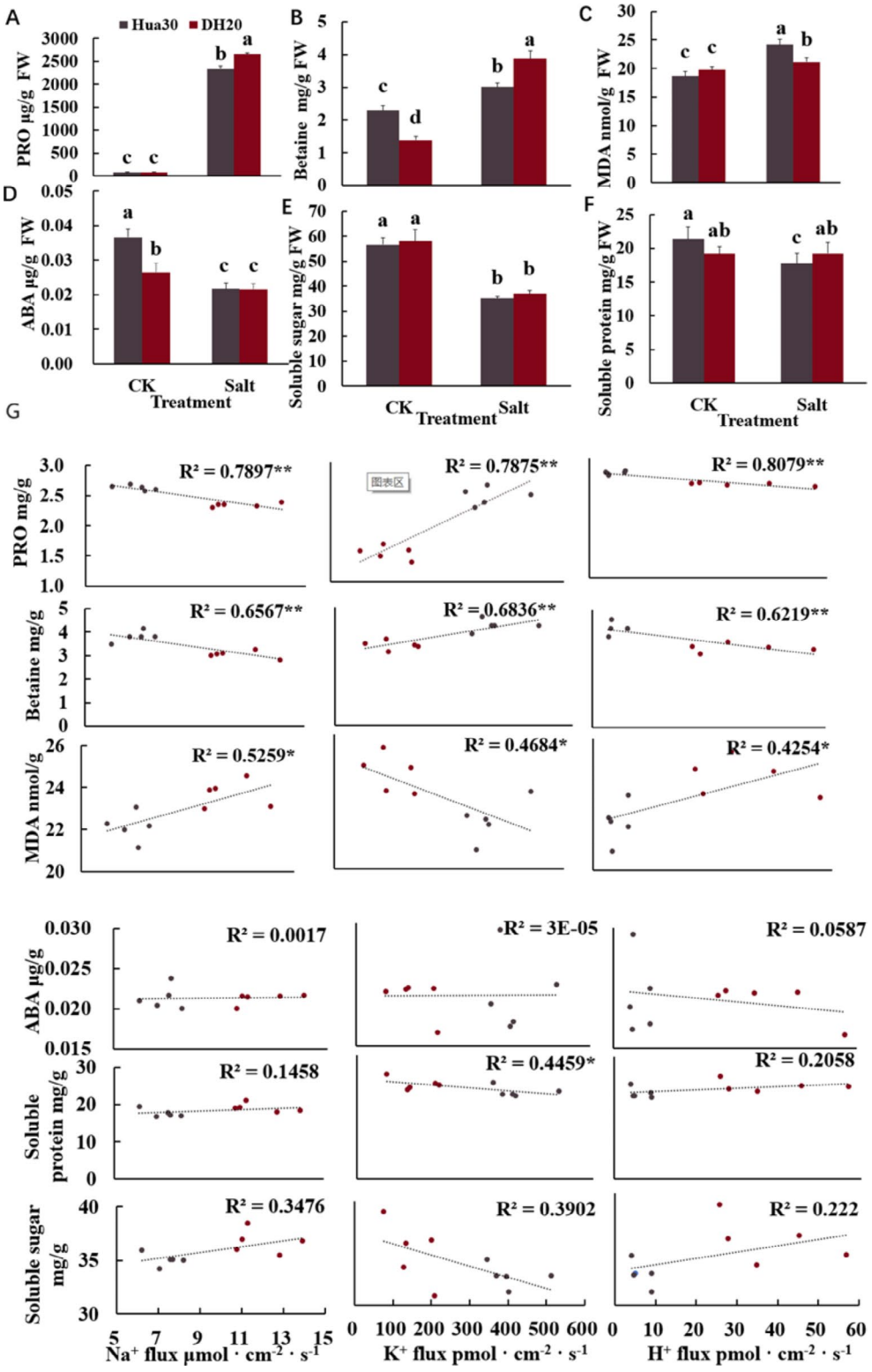

Fig. 4 Comparison of the osmolytes and ABA between Hua30 and DH20 under different treatments. **A**: PRO; **B**: Betaine; **C**: MDA; **D**: ABA; **E**: Soluble protein; **F**: Soluble sugar; **G**: Correlation among the osmolytes, ABA with the average ion efflux rates of Na^+, K^+, and H^+ in mesophyll cells after salt treatment stress for 24 h. Red dots and black dots represent DH20 and Hua30, respectively, with each dot indicating one biological replicate. Different lowercase letters denote significant differences between Hua30 and DH20 under different treatments at the 0.05 level, as determined by Fisher's least significant difference (LSD) test. Asterisks (* and **) represent a significant correlation between the two materials at the 0.05 and 0.01 levels, respectively

Effect of salt stress on the antioxidant system in Hua30 and DH20

Comparing the differences in key antioxidant enzyme activities between the two materials under salt stress, no significant differences were observed in the activities of ascorbate peroxidase (APX), catalase (CAT), peroxidase (POD), and superoxide dismutase (SOD) between Hua30 and DH20 under normal control conditions. However, in response to salt stress, the activities of APX, CAT, POD, and SOD were significantly higher in DH20 compared to Hua30 (Fig. 5A, B, C and D).

The correlation between the activities of antioxidant enzymes and the ion efflux rates of Na^+, K^+, and H^+ in mesophyll cells subjected to salt treatment was also examined. It was found that ascorbate peroxidase (APX), peroxidase (POD), and superoxide dismutase (SOD) exhibited highly significant correlations with the efflux rates of Na^+, K^+, and H^+ ions (Fig. 5E).

Comparison of the relative expression levels of *HvSOSs* gene family between Hua30 and DH20

Through the analysis of relative expression levels of the *HvSOS* gene family in the two materials, we found that the relative expression levels of the *HvSOS1* genes showed no significant difference at 0 h (Fig. 6A), but higher expression levels of *HvSOS2* and *HvSOS3* were observed in DH20 compared to Hua30 at 0 h (Fig. 6B and C). However, at 24 h, the expression levels of all three genes in DH20 were significantly lower than those in Hua30. No significant differences were observed in the expression of these three genes between the two materials at 48 h (Fig. 6A, B and C).

By comparing the relationship between the relative expression levels of *HvSOSs* and the ion efflux rates of Na^+, K^+, and H^+ under salt stress, we found that *HvSOS1*, *HvSOS2* and *HvSOS3* exhibited a highly significant correlation with the ion efflux rates of Na^+, K^+, and H^+, respectively (Fig. 6D).

Comparison of the relative expression levels of key genes in *HvHKTs* gene family between Hua30 and DH20

The expression of the key *HvHKTs* gene family was analyzed in two materials. No significant difference in the expression of *HvHKT1;1* was observed from 0 to 48 h between the two materials under different treatments (Fig. 7A). The relative expression of *HvHKT1;3* was significantly lower in DH20 at 0 h. However, after 24 and 48 h of salt treatment, the relative expression of *HvHKT1;3* in DH20 was significantly higher than that in Hua30 (Fig. 7B). At the control time point (0 h), the relative expression levels of both *HvHKT1;5* and *HvHKT2;1* in DH20 were significantly higher than those in Hua30; however, no significant differences were found between Hua30 and DH20 after 24 and 48 h of salt treatment (Fig. 7C and D). Furthermore, it was observed that the ion efflux rates of Na^+, K^+, and H^+ exhibited a highly significant correlation with *HvHKT1;3*. Additionally, *HvHKT2;1* showed a significant correlation with H^+ efflux under salt treatment (Fig. 7E).

Comparison of the relative expression levels of key genes in the *HvNHXs* gene family between Hua30 and DH20

In addition to *HvNHX2*, the relative expression levels of *HvNHX1*, *HvNHX3*, and *HvNHX5* in DH20 were significantly higher than those in Hua30 at 0 h. However, 24 h after salt treatment, lower expression levels of *HvNHX1*, *HvNHX2*, and *HvNHX3* were observed in DH20 compared to Hua30(Fig. 8A, B and C). There was no significant difference in the relative expression of *HvNHX5* between the two materials after 24 h of salt treatment (Fig. 8D). After 48 h of salt treatment, no significant differences were found for *HvNHX1* and *HvNHX2*. However, for *HvNHX3* and *HvNHX5*, the relative expression levels were higher in DH20 than in Hua30 (Fig. 8A, B, C and D). By comparing the ion efflux rate with key genes in the *HvNHXs* gene family under salt stress, we found that *HvNHX1*, *HvNHX2* and *HvNHX3* were significantly correlated with the Na^+, K^+, and H^+ ion efflux rates of the two materials (Fig. 8E).

A model describing the salt tolerance mechanism of DH20

By integrating all the findings described above, we propose a model for the salt tolerance mechanism of DH20. This model suggests that K^+ and Na^+ ion homeostasis is coordinated with other key osmolytes and antioxidant regulation to cope with salt stress (Fig. 9). No significant difference was observed in the absorption of Na^+ into the epidermal cells of roots between the two materials; however, Na^+ was loaded less into the xylem in DH20 but effluxed more in the mesophyll cells compared to Hua30, probably via the action of *HvSOS1*, *HvSOS2* and *HvSOS3*. Then, Na^+ was rapidly sequestered into leaf vacuoles via a tonoplast Na^+/H^+ exchanger (NHX), likely involving *HvNHX1*, *HvNHX2* and *HvNHX3* to achieve rapid osmotic adjustment and avoid Na^+ damage. PRO, betaine and MDA may play crucial roles in osmotic adjustment and avoiding Na^+ damage of DH20. Once Na^+ achieves its limit in the vacuole, *HKT1;3* genes may mediate limited Na^+ accumulation in shoots. At the same time, K^+ retention and H^+ efflux in leaf mesophyll constitute important components of the salinity tolerance mechanism in DH20. Higher net H^+ efflux in DH20 may be essential as a compensatory mechanism at restoring cytosolic K^+ homeostasis under salinity stress. Therefore, the increase of Na^+ efflux and K^+ concentration retention result in a higher K^+/Na^+ ratio in DH20. In addition, the average length of stomatal guard cells and chloroplast ultrastructure data show that DH20 protects photosystems from

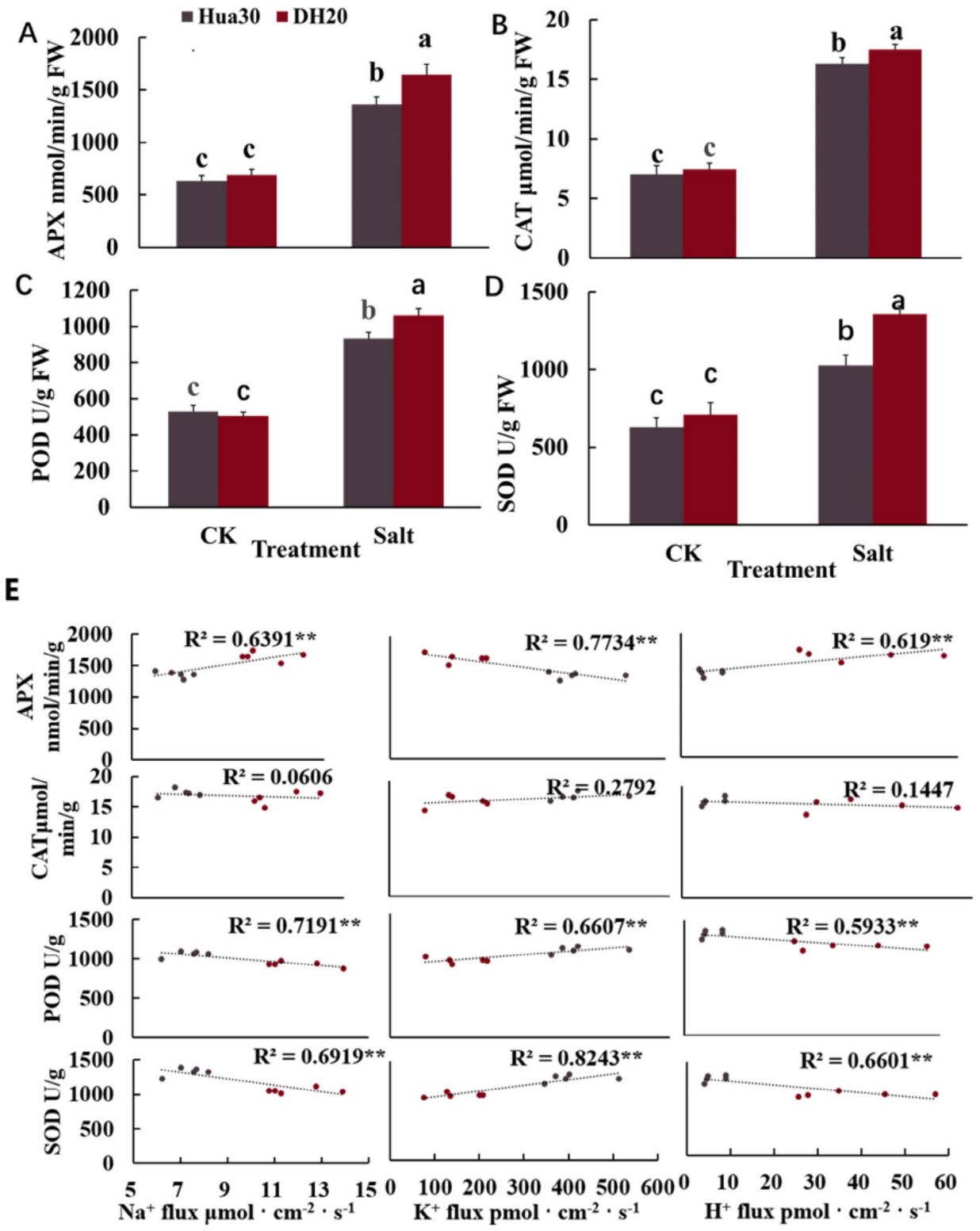

Fig. 5 Comparison of key antioxidant enzyme activities between Hua30 and DH20 under different treatments. **A**: APX; **B**: CAT; **C**: POD; **D**: SOD; **E**: Correlation among the antioxidant enzyme activities with the average ion efflux rates of Na^+, K^+, and H^+ in mesophyll cells after salt treatment for 24 h. Red dots and black dots represent DH20 and Hua30, respectively, with each dot indicating one biological replicate. Different lowercase letters denote significant differences between Hua30 and DH20 under different treatments at the 0.05 level, as determined by Fisher's least significant difference (LSD) test. Asterisks (* and **) represent a significant correlation between the two materials at the 0.05 and 0.01 levels, respectively

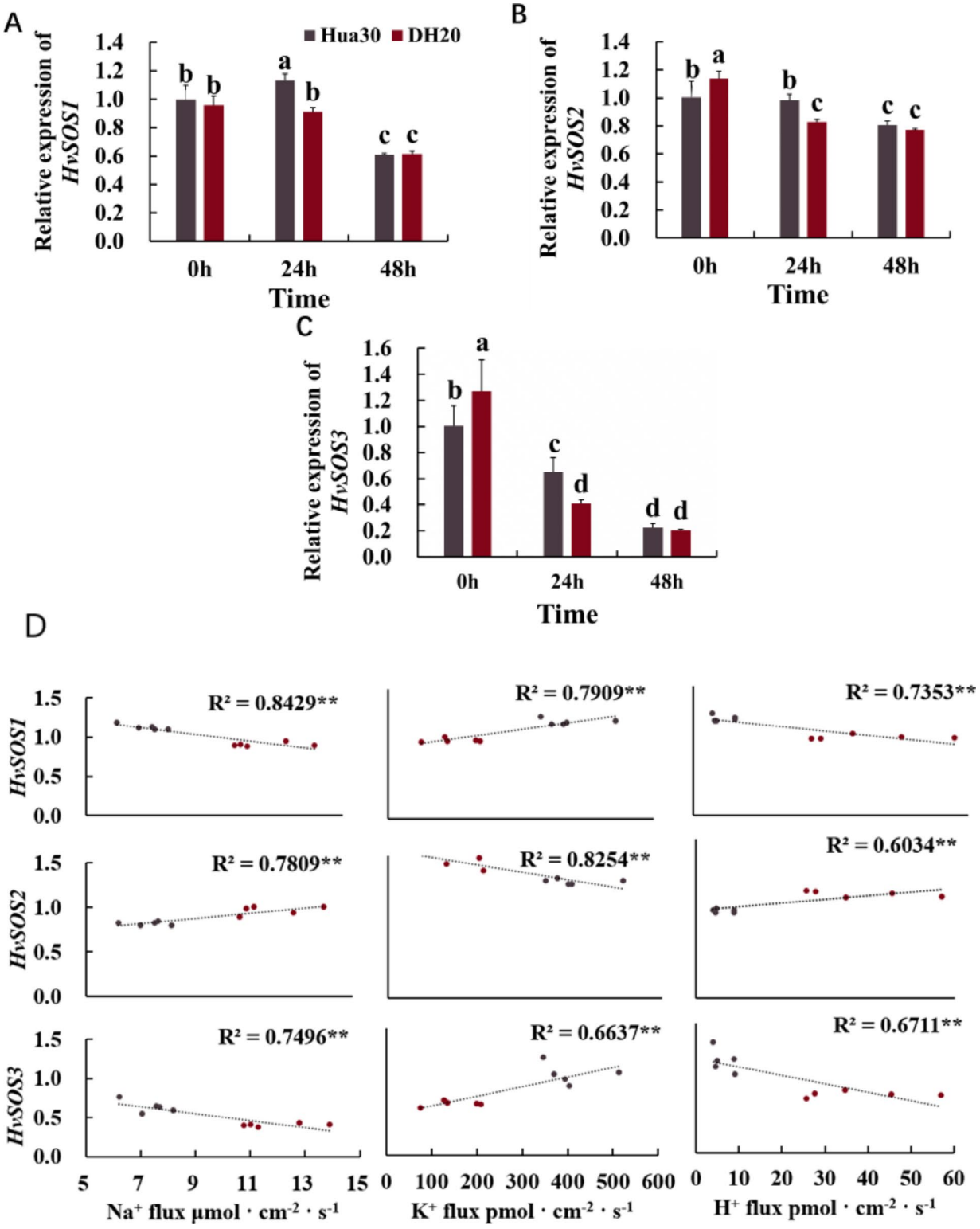

Fig. 6 Relative expression levels of *HvSOSs* gene family in DH20 and Hua30 after salt treatment. **A**: *HvSOS1*;**B**: *HvSOS2*;**C**: *HvSOS3*;**D**: Correlation between the *HvSOSs* genes with the average ion efflux rates of Na^+, K^+, and H^+ in mesophyll cells after salt stress for 24 h. Red dots and black dots represent DH20 and Hua30, respectively, with each dot indicating one biological replicate. Different lowercase letters denote significant differences between Hua30 and DH20 under different treatments at the 0.05 level, as determined by Fisher's least significant difference (LSD) test. Asterisks (* and **) represent a significant correlation between the two materials at the 0.05 and 0.01 levels, respectively

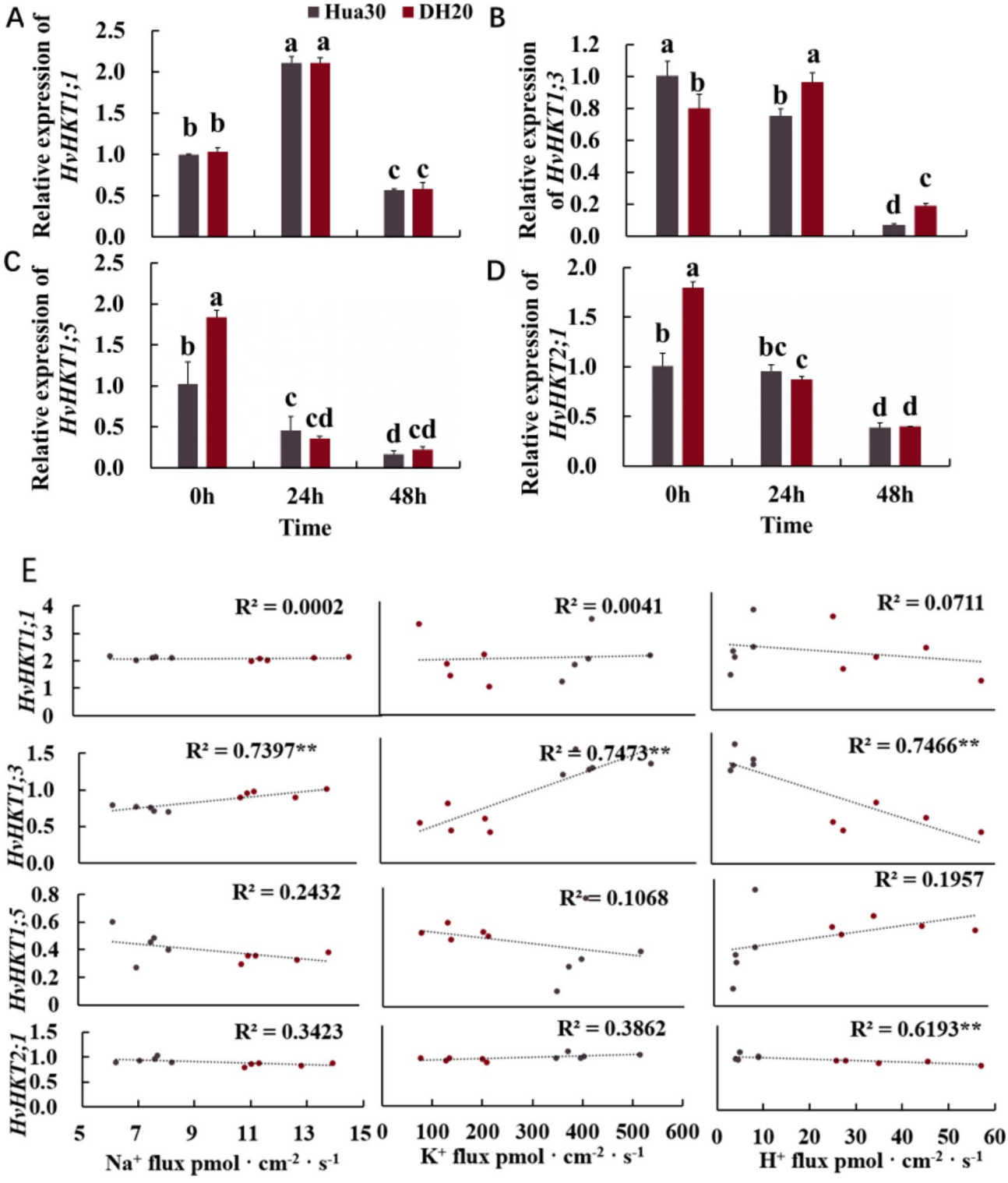

Fig. 7 Relative expression levels of *HvHKTs* gene family in DH20 and Hua30 after salt treatment. **A**: *HvHKT1;1*; **B**: *HvHKT1;3*; **C**: *HvHKT1;5*; **D**: *HvHKT2;1*;**E**: Correlation between the *HvHKTs* genes and the ion efflux rates of Na^+, K^+, and H^+ in mesophyll cells under salt stress. Red dots and black dots represent DH20 and Hua30, respectively, with each dot indicating one biological replicate. Different lowercase letters denote significant differences between Hua30 and DH20 under different treatments at the 0.05 level, as determined by Fisher's least significant difference (LSD) test. Asterisks (* and **) represent a significant correlation between the two materials at the 0.05 and 0.01 levels, respectively

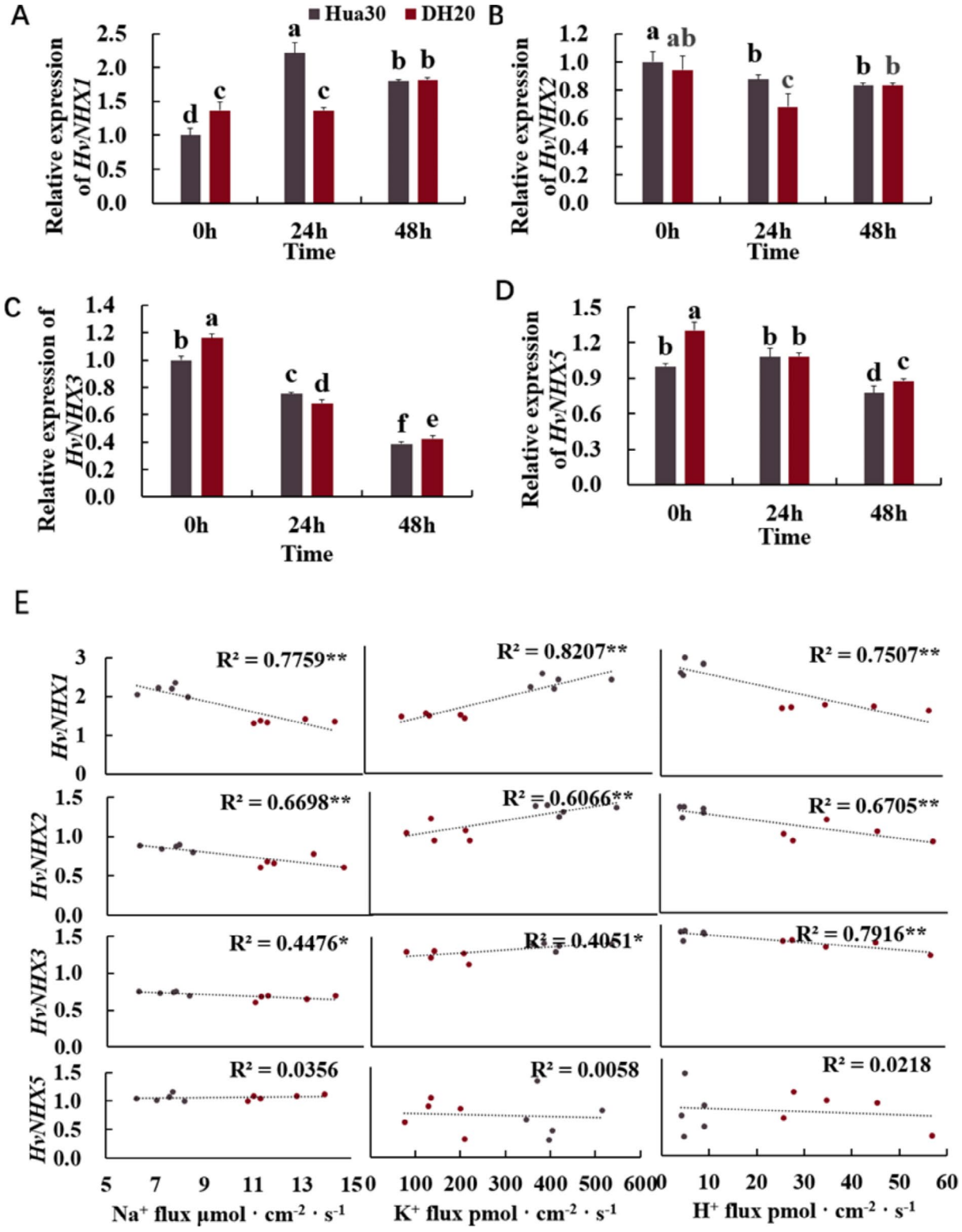

Fig. 8 Relative expression levels of *HvNHXs* gene family in DH20 and Hua30 after salt treatment. **A**: *HvNHX1*; **B**: *HvNHX2*; **C**: *HvNHX3*; **D**: *HvNHX5*;**E**: Correlation among the *HvNHXs* genes with the average ion efflux rates of Na^+, K^+, and H^+ in mesophyll cells under salt stress. Red dots and black dots represent DH20 and Hua30, respectively, with each dot indicating one biological replicate. Different lowercase letters denote significant differences between Hua30 and DH20 under different treatments at the 0.05 level, as determined by Fisher's least significant difference (LSD) test. Asterisks (* and **) represent a significant correlation between the two materials at the 0.05 and 0.01 levels, respectively

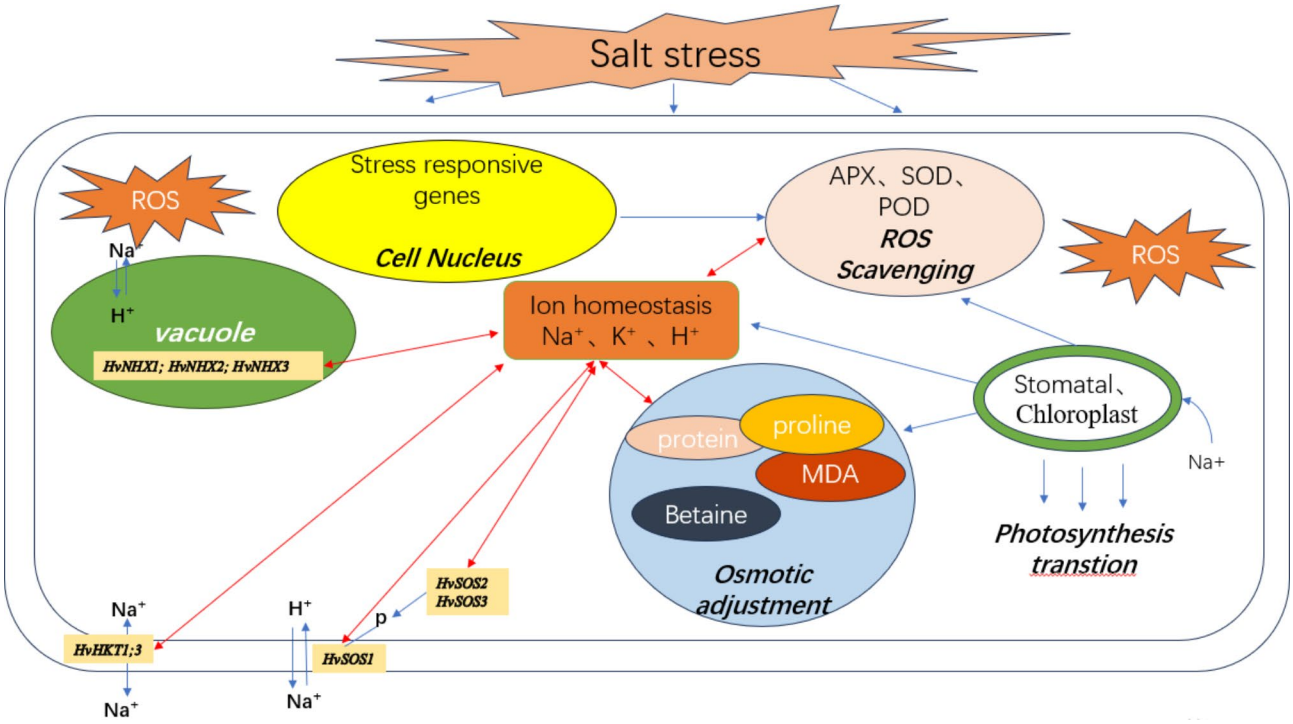

Fig. 9 A model of the salt tolerance mechanism in the leaf mesophyll cells of DH20. The red bidirectional arrow represents that the ion efflux flow rate is correlated with the corresponding indices, including the correlation between soluble protein and K^+ efflux. After 24 h of salt stress, the Na^+, K^+, and H^+ flux in the leaf mesophyll cells of DH20 is highly correlated with proline, MDA, and betaine levels. Additionally, K^+ shows a correlation with soluble protein in DH20. Regarding reactive oxygen species (ROS) scavenging, the Na^+, K^+, and H^+ fluxes are significantly correlated with the activities of APX, SOD, and POD. Furthermore, the relative expression levels of the *HvSOS1*, *HvSOS2*, *HvSOS3*, *HvHKT1;3*, *HvNHX1*, *HvNHX2*, and HvNHX3 genes, which exhibit strong correlation with Na^+, K^+, and H^+ efflux of DH20

damage caused by salt stress by enhancing antioxidant enzyme activities (APX, POD, and SOD) to scavenge more induced ROS, thereby maintaining a higher photosynthetic rate and promoting better growth and development of the plant under salt stress.

Discussion

DH20 line exhibited salt tolerance in shoot rather than in root

Previous studies have reported that a homozygous barley line (DH20), which exhibits improved salt tolerance compared to its wild type control, was rapidly generated through mutagenesis combined with microspore culture [25]. In response to salt stress, DH20 demonstrated better tolerance, as evidenced by its superior shoot fresh weight, relative growth rate and leaf K^+/Na^+ ratio compared to the original material.

In the present study, we further observed a significant increase in the fresh weight, dry weight and relative growth rate of plant height in the aboveground parts compared to the root system. Additionally, under salt stress conditions, the key photosynthetic parameters (Maximum net photosynthetic rate, Fv'/Fm' and chlorophyll content) of DH20 are superior to those of Hua30, suggesting that DH20 is more efficient in carbon assimilation under salt stress, potentially linked to stomatal factors. Further measurements of the length of stomatal guard cells revealed that the guard cell length of DH20 after salt stress treatment was significantly greater than that of the control material Hua30. An examination of the ultrastructure of chloroplasts in DH20 showed no significant plasmolysis, clear grana lamellae, and intact thylakoid structures, which effectively supports the normal progression of photosynthesis during salt stress treatment.

Sodium and potassium ion homeostasis under high salinity conditions has been highlighted as a critical factor [8]. Notably, the K^+/Na^+ ratio in the aboveground parts of DH20 under salt treatment was consistently higher than that of Hua30 [25]. Further investigation into the ion efflux currents of K^+, Na^+, and H^+ in mesophyll cells and roots utilizing NMT technology revealed that DH20 exhibited a greater capacity for K^+ retention and Na^+ efflux in the mesophyll cells. Although root xylem cells displayed a reduced ability to absorb Na^+, no significant differences were observed in the rates of Na^+ and K^+ efflux in the root epidermal cells. This is similar with the findings of Garthwaite [31], which indicate that salt tolerance in wild *Hordeum* species is associated with restricted entry of Na^+ and Cl^- into the shoots. Here, the

salt tolerance of DH20 is primarily associated with the K^+ retention, Na^+ and H^+ efflux in the mesophyll cells. K^+ is considered a limiting factor in crop yield and quality, directly affecting cell expansion and growth [32]. At the cellular level, maintaining intracellular K^+ homeostasis is important for enzyme activation, stabilization of protein synthesis, and maintenance of cytoplasmic pH homeostasis [33]. Wu et al. (2020) [34] demonstrated an increased rate of Na^+ efflux from the roots, alongside a diminished sensitivity of K^+ efflux, thereby enhancing the salt tolerance of barley. Additionally, Wang et al. (2016) [35] reported that both Na^+ efflux and K^+ influx was augmented to maintain a balance between K^+ and Na^+ during the seedling stage under prolonged salt stress in wild barley.

Key osmolytes and antioxidant enzyme activities are closely related to ion balance

Numerous studies have investigated the physiological responses in barley, while the relationship among ion flux, osmotic adjustment and oxidation resistance have been less reported. Izadi et al. (2014) [36] found that, compared to wheat, the higher K^+/Na^+ ratio, proline content, increased superoxide dismutase activity and protein content in barley may be the main factors contributing to its strong salt tolerance. Kiani et al. (2017) [37] reported that barley mutants improved their salt tolerance mainly by removing reactive oxygen species and maintaining cell ion homeostasis. Ahmed et al. [38] showed that the increased levels of K^+ content, K^+/Na^+ ratio, ATPase activity, betaine content, proline content and antioxidant capacity under salt stress were the main reasons for salt tolerance of Tibetan barley [38]. In this study, APX, POD, and SOD exhibited a highly significant correlation with the efflux rates of Na^+, K^+, and H^+ ions in the mesophyll cells. Dong et al. (2024) [39] suggested that the exogenous addition of betaine significantly enhances the salt tolerance of *Glycyrrhiza uralensis* seedlings by increasing antioxidant enzyme activities. Plants have developed special scavenging systems to avoid the negative effects of reactive oxygen species. Enhancing antioxidant metabolism to scavenge ROS is very important to enable plants to resist salt stress. The key elements of these processes are enzymes that catalyze metabolic reactions, such as APX, POD and POD, which are important antioxidant enzymes involved in plant salt tolerance [39].

To adapt to osmotic stress, plants not only enhance the activity of antioxidant enzymes but also accumulate compatible osmolytes, which helps to maintain cellular water potential and membrane stability [6]. This study found that proline, betaine, and malondialdehyde (MDA) exhibited a significant correlation with ion homeostasis. Notably, soluble proteins were found to be correlated with K^+ efflux. This indicates that proline, betaine, MDA, and soluble protein content play crucial roles in the response of DH20 to salt stress, suggesting that DH20 possesses a greater capacity to maintain normal osmotic balance and withstand adverse conditions. Some studies have demonstrated positive correlation between proline content and salt tolerance [40]. For instance, the proline content in cabbage increases under salt stress, enhancing its adaptability to such conditions [41]. After salt stress treatment, the content of free proline in shoots of salt-tolerant cultivar potato increased [40], and salt-tolerant rice varieties exhibit higher proline content compared to sensitive varieties [42]. Yu et al. (2022) revealed that the betaine content in wheat is linked to its salt tolerance and identified a TaBADH-A1 allele that may enhance salt tolerance [43]. Other studies have indicated that the MDA content in salt-tolerant wheat varieties is lower than that in sensitive varieties, suggesting that the cell membrane quality in sensitive wheat leaves is inferior to that in salt-tolerant varieties, necessitating higher MDA levels to maintain homeostasis [44]. Furthermore, prior research indicates that salt stress adversely affects the protein synthesis pathway, accelerating protein hydrolysis and leading to a substantial accumulation of amino acids, which ultimately results in a reduction in protein content of rice [45]. In this study, the K^+ efflux rate exhibited a significant correlation with soluble protein levels. This finding suggests that the accumulation of soluble proteins in DH20 not only supports osmotic regulation mechanisms to maintain water balance within plants but also enhances K^+ homeostasis, thereby contributing to their salt tolerance. It is suggested that these osmotic and antioxidant enzymes could help the ion homeostasis in DH20 response to the salt stress.

Key genes regulate ion transport, compartmentalization and distribution

In response to salt stress, plants mainly regulate the ion transport, compartmentalization and distribution through the multiple genes, especially including the classic *HvSOSs*, *HvHKTs*, and *HvNHXs* gene families [46, 47]. Here, the relative expression of the *HvSOS1*, *HvSOS2* and *HvSOS3* genes in DH20 was significantly higher than that in Hua30 after 24 h of salt stress treatment. Furthermore, we found that expression of *HvSOS1*, *HvSOS2* and *HvSOS3* was highly significantly correlated with the ion efflux rates of Na^+, K^+, and H^+ in the mesophyll cells, respectively (Fig. 6D). Numerous studies have highlighted the crucial role of *HvSOS1* in the Na + compartmentalization and its loading into the xylem [48]. To our knowledge, the correlation between the expression of *HvSOS2* and *HvSOS3* in the shoot and ion flux has not yet been reported.

The HKT transporter plays a crucial role in the regulation of Na^+ homeostasis by mediating Na^+-specific

transport or Na^+-K^+ transport [49]. Currently, members of the HKT gene family have been cloned from various plants, including Arabidopsis [50], rice [51], wheat [52] and barley [53]. The transfer of Na^+ from roots to shoots and the accumulation of K^+ in stems mediated by *HKT* family genes (ZmHKT1 and ZmHKT2) in maize are important strategies for enhancing salt tolerance in maize [54]. It has been found that barley *HKT1;1* is mainly responsible for returning Na^+ from the shoot to the root, while *HKT1;5* is responsible for transporting Na^+ from the root to the shoot [55]. In bread wheat, the TaHKT1;5 (L190P) was associated with reduced Na^+ retrieval from the xylem and elevated shoot Na^+ accumulation [55]. The over-expression of *HvHKT2;1* enhances salt tolerance by promoting the salt-accumulating behavior of barley [53]. Conversely, a decrease in the expression level of *TaHKT2;1* in transgenic wheat resulted in diminished root Na^+ uptake and reduced translocation into the xylem sap, thereby improving tolerance to salinity [52]. In this study, compared to Hua30, the expression of *HvHKT1;3* genes in salt-treated DH20 increased significantly, which may be related to the enhanced Na^+ efflux from the shoot of DH20.

Under salt stress, Na^+/H^+ exchangers (NHXs) play a critical role in intracellular potassium transport and the maintenance of membrane PH [56]. Studies have demonstrated that K^+ content decreases while Na^+ content increases in the leaf tissue vacuole of the nhx1 nhx2 double mutant under salt stress [57]. The Arabidopsis nhx5 nhx6 mutant exhibits salt sensitivity, indicating that *AtNHX5* and *AtNHX6* are essential for vesicle trafficking and stress response in Arabidopsis [58]. Chen et al. (2015) found that overexpression of the *SeNHX1* gene in marine plants enhanced the sequestration of Na^+ into the vacuole under salt stress, thereby improving the salt tolerance of tobacco [59]. Research has indicated that the upregulation of the *NHXs* gene family under salt stress facilitates the efflux of Na^+ and plays a vital role in maintaining ion homeostasis in salt-tolerant genotypes [58, 59]. In this study, *HvNHX1*, *HvNHX2*, and *HvNHX3* exhibited a highly significant correlation with Na^+, K^+, and H^+ ion efflux rates, suggesting that these three genes may play a pivotal role in enhancing the compartmentalization of Na^+ into the vacuole and the efflux of Na^+ in mesophyll cells. This study elucidates the correlation between various physiological, molecular indicators and ion flux in mesophyll cells at a critical time point in barley. Future research would benefit from conducting dynamic comparisons and analyses at multiple time points during salt treatment.

Genetic engineering and breeding applications aimed at improving salt tolerance by improving ion homeostasis mechanisms have attracted considerable attention in recent years [60]. Here, the mechanisms by which these genes(*HvSOS1*, *HvSOS2*, *HvSOS3*, *HvHKT1;3*, *HvNHX1*, *HvNHX2*, and *HvNHX3*) regulate ion homeostasis in DH20 by genetic engineering merit further exploration and could be applied to future breeding efforts. Breeding salt tolerance in crops using genetic engineering depends largely on the availability of salt-tolerant genetic resources, reliable screening techniques, identification of salt-tolerant genetic components, and successful genetic manipulation of the required genetic background [61]. The main genes modified by researchers include those encoding: (1) osmotic compatibility (glycine betaine, proline, sugar, etc.), (2) transcription factors (dehydration response binding protein and MYB transcription factor), and (3) enzymatic and non-enzymatic rich in antioxidants (ascorbate peroxidase, glutamine synthetase), (4) ion transporters (NHX1, AVP1, HAL1), (5) protein genetic engineering heat shock and late embryonic development (LEA) [60]. By utilizing advanced breeding techniquesQTL, MAS, high-throughput genotyping, multigene approach, RNAi, transposon insertional knockouts and CRISPR/Cas9 gene editing, researchers and breeders can create crop varieties that are better equipped to thrive in saline environments [61].

In summary, while wheat, rice, and barley share common strategies for managing salt stress, their approaches to ion homeostasis and coordinated salt tolerance mechanisms differ significantly [8, 62]. A strong correlation exists between a plant's ability to retain K^+ and its salinity tolerance in both the leaves and roots of barley and wheat; however, the pathways of K^+ leakage from both root and leaf tissues vary substantially between these two species [8]. Wheat focuses on K^+ retention and Na^+ exclusion through specific transporters. For instance, the transporter TaHKT1;5 has been identified as crucial for Na^+ retrieval from the xylem, thereby preventing excessive Na^+ from reaching the leaves, which is vital for maintaining photosynthetic efficiency and overall plant health [63]. Additionally, wheat utilizes vacuolar Na^+ sequestration mechanisms, where Na^+ is compartmentalized in vacuoles to mitigate its toxic effects [64]. Rice relies heavily on the SOS pathway for Na^+ management. The SOS1 gene encodes a Na^+/H^+ antiporter that actively extrudes Na^+ from root cells into the apoplast, thus preventing its accumulation in the cytoplasm [65]. Rice also employs vacuolar Na^+ sequestration through NHX transporters, which help in compartmentalizing Na^+ in vacuoles, thereby maintaining ionic balance and turgor pressure [66]. Barley combines effective ion sequestration with robust antioxidant responses [1], where ROS-induced K^+ leakage may become increasingly significant, potentially explaining the generally higher salt sensitivity of wheat compared to barley [8]. Understanding these differences is crucial for breeding programs aimed at enhancing salt tolerance in these essential crops, especially in the face of increasing soil salinization and climate change challenges.

Conclusion

The physiological and molecular mechanisms underlying salt tolerance in the barley doubled haploid (DH) line DH20, derived from mutagenesis combined with microspore culture, were elucidated. It is suggested that key osmolytes, antioxidant enzyme activities, and associated gene expression play a vital role in improving ion homeostasis in DH20 under salt stress in mesophyll cells. The retention of K^+ ions, along with the efflux of Na^+ and H^+ ions, has been identified as crucial mechanisms enabling this DH line to cope with salt stress. These findings may serve as a foundation for the rapid breeding of new salt-tolerant cultivars.

Supplementary Information

The online version contains supplementary material available at https://doi.org/10.1186/s12870-024-06033-0.

Supplementary Material 1

Acknowledgements
Not applicable.

Author contributions
HX wrote the paper and produced the figures and tables. HC, TH and BY performed the experiment. LZ analyzed the data. RX and NGH improved the manuscript. CL and HG conceived and designed the experiments. All authors read and approved the final version of manuscript.

Funding
This work was supported by the Natural Science Foundation of Shanghai (22ZR1444900); SAAS Program for Excellent Research Team (2022(018)); China Agriculture Research System of MOF and MARA (Grant CARS-05–01 A-02); NGH is supported at Rothamsted Research by the United Kingdom's Biotechnology and Biological Sciences Research Council (BBSRC) via the Designing Future Wheat Programme (BB/P016855/1).

Data availability
Data is provided within the manuscript and supplementary information files.

Declarations

Ethics approval and consent to participate
Not applicable.

Consent for publication
Not applicable.

Competing interests
The authors declare no competing interests.

Author details
[1]Shanghai Key Laboratory of Agricultural Genetics and Breeding, Key Laboratory for Safety Assessment (Environment) of Agricultural Genetically Modified Organisms of Ministry of Agriculture and Rural Affairs (Shanghai), Biotechnology Research Institute of Shanghai Academy of Agricultural Sciences, Shanghai 201106, China
[2]Rothamsted Research, Harpenden AL5 2JQ, UK
[3]Yangzhou University, Yangzhou 225009, China

Received: 11 October 2024 / Accepted: 30 December 2024
Published online: 14 January 2025

References

1. Gharaghanipor N, Arzani A, Rahimmalek M, Ravash R. Physiological and transcriptome indicators of salt tolerance in wild and cultivated barley. Front Plant Sci. 2022;13:819282.
2. Urbanavičiūtė I, Bonfiglioli L, Pagnotta MA. One hundred candidate genes and their roles in drought and salt tolerance in wheat. Int J Mol Sci. 2021;22:6378.
3. Zhang J, Jiang J, Shan Q, Chen G, Wang Y, Shen L, Pan C, Wu H, Abarquez A. Soil salinization and ecological remediation by planting trees in China. In: Inter Conf Mech Auto Control Engi. Wuhan, China, 26–28 June 2010; IEEE: Piscataway, NJ, USA, 2010;1349–52.
4. Cui YR, Zhang F, Zhou YL. The application of Multi-locus GWAS for the detection of salt-tolerance loci in rice. Front Plant Sci. 2018;9:1464.
5. Wu HH, Shabala L, Zhou MX, Su N, Wu Q, Ul-Haq T, Zhu J, Mancuso S, Azzarello E, Shabala S. Root vacuolar Na^+ sequestration but not exclusion from uptake correlates with barley salt tolerance. Plant J. 2019;100(1):55–67.
6. Munns R, Tester M. Mechanisms of salinity tolerance. Annu Rev Plant Biol. 2008;59:651–81.
7. Van Zelm E, Zhang Y, Testerink C. Salt tolerance mechanisms of plants. Annu Rev Plant Biol. 2020;71:403–33.
8. Wu HH, Shabala L, Barry K, Zhou MX, Shabala S. Ability of leaf mesophyll to retain potassium correlates with salinity tolerance in wheat and barley. Physiol Plant. 2013;149(4):515–27.
9. Liu BH, Zhang JH, Ye NH. Noninvasive micro-test technology: monitoring ion and molecular flow in plants. Trends Plant Sci. 2023;28(1):123–4.
10. Wang H, Shabala L, Zhou M, Shabala S. Hydrogen peroxide-induced root Ca^{2+} and K^+ fluxes correlate with salt tolerance in cereals: towards the cell-based phenotyping. Int J Mol Sci. 2018;19:702.
11. Wang H, Shabala L, Zhou M, Shabala S. Developing a high-throughput phenotyping method for oxidative stress tolerance in barley roots. Plant Methods. 2019;15:12.
12. Shabala S, Shabala L, Volkenburgh EV. Effect of calcium on root development and root ion fluxes in salinised barley seedlings. Funct Plant Biol. 2003;30(5):507–14.
13. Velarde-Buendía AM, Shabala S, Cvikrova M, Dobrovinskaya O, Pottosin I. Salt-sensitive and salt-tolerant barley varieties differ in the extent of potentiation of the ROS-induced K^+ efflux by polyamines. Plant Physiol Biochem. 2012;61:18–23.
14. Cuin TA, Shabala S. Amino acids regulate salinity-induced potassium efflux in barley root epidermis. Planta. 2007;225(3):753–61.
15. Azhar N, Su N, Shabala L, Shabala S. Exogenously Applied 24-Epibrassinolide (EBL) ameliorates detrimental effects of Salinity by reducing K^+ efflux via depolarization-activated K^+ channels. Plant Cell Physiol. 2017;58(4):802–10.
16. Shabala S, Shabala S, Cuin TA, Pang J, Percey W, Chen Z, Conn S, Eing C, Wegner LH. Xylem ionic relations and salinity tolerance in barley. Plant J. 2010;61(5):839–53.
17. Han Y, Yin SY, Huang L, Wu XL, Zeng JB, Liu XH, Qiu L, Munns R, Chen ZH, Zhang GP. A sodium transporter HvHKT1;1 confers salt tolerance in barley via regulating tissue and cell ion homeostasis. Plant Cell Physiol. 2018;59(10):1976–89.
18. Fu LB, Wu DZ, Zhang XC, Xu YF, Kuang LH, Cai SG, Zhang GP, Shen QF. Vacuolar H^+-pyrophosphatase HVP10 enhances salt tolerance via promoting Na^+ translocation into root vacuoles. Plant Physiol. 2022;188(2):1248–63.
19. Wu HH, Zhu M, Shabala L, Zhou MX, Shabala S. K^+ retention in leaf mesophyll, an overlooked component of salinity tolerance mechanism: a case study for barley. J Integr Plant Biol. 2015;57(2):171–85.
20. Li HS, Li SX, Abdelkhalik S, Shahzad A, Gu J, Yang ZH, Ding ML, Liu K, Zhao H, Yang MJ. Development of thermo-photo sensitive genic male sterile lines in wheat using doubled haploid breeding. BMC Plant Biol. 2020;20(1):246.
21. Wu MF, Goldshmidt A, Ovadya D, Larue H. I am all ears: maximize maize doubled haploid success by promoting axillary branch elongation. Plant Direct. 2020;4(5):e00226.
22. Meng D, Liu C, Chen S, Jin W. Haploid induction and its application in maize breeding. Mol Breed. 2021;41(3):20.
23. Forster BP, Thomas WTB. Doubled haploids in genetics and plant breeding. Plant Breed Rev. 2005;25:57–88.
24. Gao RH, Guo GM, Fang CY, Huang SH, Chen JM, Lu RJ, Huang JH, Fan XR, Liu CH. Rapid generation of barley mutant lines with high nitrogen uptake efficiency by microspore mutagenesis and field screening. Front Plant Sci. 2018;9:450.
25. Xu HW, Halford NG, Guo GM, Chen ZW, Li YB, Zhou LH, Liu CH, Xu RG. Transcriptomic and metabolomic analyses reveal the importance of lipid

metabolism and photosynthesis regulation in high salinity tolerance in barley (*Hordeum vulgare* L.) leaves derived from mutagenesis combined with microspore culture. Int J Mol Sci. 2023;24(23):16757.
26. Li Q, Zhou LY, Chen Y, Xiao N, Zhang DP, Zhang MJ, Wang WG, Zhang CQ, Zhang AN, Li H, Chen JM, Gao Y. Phytochrome interacting factor regulates stomatal aperture by coordinating red light and abscisic acid. Plant Cell. 2022;34(11):4293–312.
27. Moussa HR, El-Gamal SM. Effect of salicylic acid pretreatment on cadmium toxicity in wheat. Biol Plant. 2010;54(2):315–20.
28. Zeng P, Xie T, Shen J, Liang T, Yin L, Liu K, He Y, Chen M, Tang H, Chen S, Shabala S, Zhang H, Cheng J. Potassium transporter OsHAK9 regulates seed germination under salt stress by preventing gibberellin degradation through mediating OsGA2ox7 in rice. J Integr Plant Biol. 2024;66(4):731–48.
29. Livak KJ, Schmittgen TD. Analysis of relative gene expression data using real-time quantitative PCR and the 2(-Delta Delta C(T)) method. Methods. 2001;25(4):402–8.
30. Meier U. A note on the power of Fisher's least significant difference procedure. Pharm Stat. 2006;5(4):253–63.
31. Garthwaite AJ, Von Bothmer R, Colmer TD. Salt tolerance in wild Hordeum species is associated with restricted entry of Na^+ and Cl^- into the shoots. J Exp Bot. 2005;56(419):2365–78.
32. Dreyer I, Uozumi N. Potassium channels in plant cells. FEBS J. 2011;278(22):4293–303.
33. Shabala S. Regulation of potassium transport in leaves: from molecular to tissue level. Ann Bot. 2003;92(5):627–34.
34. Wu Q, Su N, Shabala L, Huang LP, Yu M, Shabala S. Understanding the mechanistic basis of ameliorating effects of hydrogen rich water on salinity tolerance in barley. Environ Exp Bot. 2020;177:104136.
35. Wang CM, Xia ZR, Wu GQ, Yuan HJ, Wang XR, Li JH, Tian FP, Zhang Q, Zhu XQ, He JJ, Kumar T, Wang XL, Zhang JL. The coordinated regulation of Na^+ and K^+ in Hordeum brevisubulatum responding to time of salt stress. Plant Sci. 2016; 252:358–366.
36. Izadi MH, Rabbani J, Emam Y, Pessarakli M, Tahmasebi A. Effects of salinity stress on physiological performance of various wheat and barley cultivars. J Plant Nutr. 2014;37(4):520 – 31.
37. Kiani D, Soltanloo H, Ramezanpour SS, Nasrolahnezhad Qumi AA, Yamchi A, Zaynali Nezhad K, Tavakol E. A barley mutant with improved salt tolerance through ion homeostasis and ROS scavenging under salt stress. Acta Physiol Plant. 2017;39(3):90.
38. Ahmed IM, Dai HX, Zheng WT, Cao FB, Zhang GP, Sun DF, Wu FB. Genotypic differences in physiological characteristics in the tolerance to drought and salinity combined stress between tibetan wild and cultivated barley. Plant Physiol Biochem. 2013;63:49–60.
39. Dong XP, Ma XM, Zhao ZL, Ma M. Exogenous betaine enhances salt tolerance of *Glycyrrhiza uralensis* through multiple pathways. BMC Plant Biol. 2024;24:165.
40. Aghaei K, Ehsanpour AA, Komatsu S. Proteome analysis of potato under salt stress. J Proteome Res. 2008;7(11):4858–68.
41. Yan L, Lu M, Riaz M, Gao G, Tong KQ, Yu HL, Wang L, Wang L, Cui KP, Wang JH, Niu YS. Differential response of proline metabolism defense, Na^+ absorption and deposition to salt stress in salt-tolerant and salt-sensitive rapeseed (Brassica napus L.) genotypes. Physiol Plant. 2024;176(4):e14460.
42. Koc YE, Aycan M, Mitsui T. Exogenous proline suppresses endogenous proline and proline-production genes but improves the salinity tolerance capacity of salt-sensitive rice by stimulating antioxidant mechanisms and photosynthesis. Plant Physiol Biochem. 2024;214:108914.
43. Yu M, Yu Y, Guo SH, Zhang MF, Li N, Zhang SX, Zhou HW, Wei F, Song TQ, Cheng J, Fan Q, Shi CY, Feng WH, Wang YK, Xiang JS, Zhang XK. Identification of *TaBADH-A1* allele for improving drought resistance and salt tolerance in wheat (*Triticum aestivum* L). Front Plant Sci. 2022;13:942359.
44. Kumar S, Beena AS, Awana M, Singh A. Physiological, biochemical, epigenetic and molecular analyses of wheat (*Triticum aestivum*) genotypes with contrasting salt tolerance. Front Plant Sci. 2017;8:1151.
45. Mandal MP, Singh RA. Influence of salinity on protein, amino acids and proline in rice seedlings. Madras Agric J. 2002;89:118–9.
46. Ismail AM, Horie T. Genomics, physiology, and molecular breeding approaches for improving salt tolerance. Annu Rev Plant Biol. 2017;68:405–34.
47. Yang Y, Guo Y. Elucidating the molecular mechanisms mediating plant salt-stress responses. New Phytol. 2017;217(2):523–39.
48. Jadidi O, Etminan A, Azizi-Nezhad R, Ebrahimi A, Pour-Aboughadareh A. Physiological and molecular responses of barley genotypes to salinity stress. Genes. 2022;13(11):2040.
49. Rodrı´guez-Navarro A, Rubio F. High-affinity potassium and sodium transport systems in plants. J Exp Bot. 2006;57:1149–60.
50. Hauser F, Horie T. A conserved primary salt tolerance mechanism mediated by HKT transporters: a mechanism for sodium exclusion and maintenance of high K(+)/Na(+) ratio in leaves during salinity stress. Plant Cell Environ. 2010;33(4):552–65.
51. Jabnoune M, Espeout S, Mieulet D, Fizames C, Verdeil JL, Conéjéro G, Rodríguez-Navarro A, Sentenac H, Guiderdoni E, Abdelly C, Véry AA. Diversity in expression patterns and functional properties in the rice HKT transporter family. Plant Physiol. 2009;150(4):1955–71.
52. Laurie S, Feeney KA, Maathuis FJ, Heard PJ, Brown SJ, Leigh RA. A role for HKT1 in sodium uptake by wheat roots. Plant J. 2002;32(2):139-49.53.
53. Mian A, Oomen RJ, Isayenkov S, Sentenac H, Maathuis FJ, Véry AA. Over-expression of an Na^+-and K^+-permeable HKT transporter in barley improves salt tolerance. Plant J. 2011;68(3):468 – 79.
54. Zhang M, Li YD, Liang XY, Lu MH, Lai JS, Song WB, Jiang CF. A teosinte-derived allele of an HKT1 family sodium transporter improves salt tolerance in maize. Plant Biotechnol J. 2023;21(1):97–108.
55. Houston K, Qiu J, Wege S, Hrmova M, Oakey H, Qu Y, Smith P, Situmorang A, Macaulay M, Flis P, et al. Barley sodium content is regulated by natural variants of the na(+) transporter HvHKT1;5. Commun Biol. 2020;3(1):258.
56. Rodríguez-Rosales MP, Gálvez FJ, Huertas R, Aranda MN, Baghour M, Cagnac O, Venema K. Plant NHX cation/proton antiporters. Plant Signal Behav. 2009;4(4):265–76.
57. Barragán V, Leidi EO, Andrés Z, Rubio L, De Luca A, Fernández JA, Cubero B, Pardo JM. Ion exchangers NHX1 and NHX2 mediate active potassium uptake into vacuoles to regulate cell turgor and stomatal function in Arabidopsis. Plant Cell. 2012;24(3):1127–42.
58. Bassil E, Ohto MA, Esumi T, Tajima H, Zhu Z, Cagnac O, Belmonte M, Peleg Z, Yamaguchi T, Blumwald E. The Arabidopsis intracellular Na^+/H^+ antiporters NHX5 and NHX6 are endosome associated and necessary for plant growth and development. Plant Cell. 2011;23(1):224–39.
59. Chen XY, Bao H, Guo J, Jia WT, Li YX. Overexpression of SeNHX1 improves both salt tolerance and disease resistance in tobacco. Plant Signal Behav. 2015;10(4):e993240.
60. Ashraf M, Athar HR, Harris PJC, Kwon TR. Some prospective strategies for improving crop salt tolerance. Adv Agron. 2008;97:45–110.
61. Arzani A, Ashraf M. Smart engineering of genetic resources for enhanced salinity tolerance in crop plants. CRC Crit Rev Plant Sci. 2016;35:146–89.
62. Craig Plett D, Møller IS. Na(+) transport in glycophytic plants: what we know and would like to know. Plant Cell Environ. 2010;33(4):612–26.
63. Chen JF, Liu Y, Zhang TY, Zhou ZF, Huang JY, Zhou T, Hua YP. Integrated physiological and transcriptional dissection reveals the core genes involving nutrient transport and osmoregulatory substance biosynthesis in allohexaploid wheat seedlings under salt stress. BMC Plant Biol. 2022;22(1):502.
64. Wu H, Shabala L, Liu X, Azzarello E, Zhou M, Pandolfi C, Chen ZH, Bose J, Mancuso S, Shabala S. Linking salinity stress tolerance with tissue-specific na (+) sequestration in wheat roots. Front Plant Sci. 2015;6:71.
67. Shahzad B, Shabala L, Zhou M, Venkataraman G, Solis CA, Page D, Chen ZH, Shabala S. Comparing essentiality of SOS1-mediated Na^+ exclusion in salinity tolerance between cultivated and wild rice species. Int J Mol Sci. 2022;23:9900.
68. Solis CA, Yong MT, Zhou M, Venkataraman G, Shabala L, Holford P, Shabala S, Chen ZH. Evolutionary significance of NHX Family and NHX1 in salinity stress adaptation in the Genus *Oryza*. Int J Mol Sci. 2022;23(4):2092.

Publisher's note